Short communication

Synthesis of oxyanion-doped barium strontium cobalt ferrites: Stabilization of the cubic perovskite and enhancement in conductivity

Jose M. Porras-Vazquez[*], Peter R. Slater

School of Chemistry, University of Birmingham, Birmingham B15 2TT, UK

ABSTRACT

In this paper we demonstrate the successful incorporation of oxyanions (borate, phosphate) into $Ba_{1-y}Sr_yCo_{0.8}Fe_{0.2}O_{3-\delta}$ (BSCF) cathode materials. For low levels of dopant, a small enhancement in the conductivity was observed; e.g. 31.6, 34.4 and 35.9 S cm^{-1} for $Ba_{0.33}Sr_{0.67}Co_{0.8}Fe_{0.2}O_{3-\delta}$, $Ba_{0.33}Sr_{0.67}Co_{0.76}Fe_{0.19}B_{0.05}O_{3-\delta}$ and $Ba_{0.33}Sr_{0.67}Co_{0.76}Fe_{0.19}P_{0.05}O_{3-\delta}$, respectively, at 700 °C. Most significantly, oxyanion doping was shown to improve the stability of the cubic form of BSCF at intermediate temperatures (especially for P-doping), helping to prevent the transition to a hexagonal cell, and maintaining its excellent electrical properties. The work shows the potential of oxyanion doping strategies to modify the performance of SOFC cathode materials.

© 2012 Elsevier B.V. All rights reserved.

1. Introduction

Research into new electrode materials for use in solid oxide fuel cells (SOFCs) has been dominated by materials with the perovskite structure, due to their generally high electronic conductivities and catalytic activity [1,2]. Although $La_{1-x}Sr_xMnO_{3-\delta}$ (LSM) is commonly used as a cathode in high temperature SOFC [3–6], it cannot be used for intermediate temperature solid oxide fuel cells (IT-SOFCs) operating at <800 °C as the activation polarization of LSM increases considerably with decreasing temperature [7].

Mixed Fe/Co perovskites have attracted great interest, such as $Ba_ySr_{1-y}Co_{0.8}Fe_{0.2}O_{3-\delta}$ perovskites (BSCF). These latter phases are among the most promising oxygen permeable membrane materials [8–12], with very high oxygen transport rates related to the high concentrations of mobile oxygen vacancies at elevated temperatures. However, cubic BSCF is a metastable compound at SOFC operating temperatures, and gradually transforms to a hexagonal perovskite that is detrimental to applications incorporating BSCF [13].

As can be seen in the above cathode systems, traditionally doping strategies have involved the partial substitution with aliovalent cations with similar size, e.g. Sr doping for La in $LaMnO_3$. Recently we have proposed an alternative doping strategy for perovskite systems with potential applications in SOFCs, namely the introduction of oxyanions (e.g. silicate, phosphate, sulfate, and borate).

Our initial work with this doping strategy targeted electrolyte systems, showing that phosphate, silicate and sulfate could be introduced into the ionic conductors $Ba_2(In/Sc)_2O_5$ leading to a structural change from brownmillerite, containing ordered oxide ion vacancies, to a cubic perovskite, where the oxide ion vacancies are disordered [14–17]. As a consequence of the resultant oxide ion disorder, an increase in the conductivity below 800 °C was observed. In other recent work, we reported the successful incorporation of silicate, phosphate and sulfate into cathode materials with $SrMO_3$ stoichiometry (M = Co, Mn), leading to a structural change from a hexagonal to a cubic perovskite and a large enhancement in the electronic conductivity [18,19]. Here we extend this work to barium strontium cobalt ferrite-based materials, $Ba_{1-y}Sr_yCo_{0.8(1-x)}Fe_{0.2(1-x)}M_xO_{3-\delta}$, investigating possible incorporation of oxyanions into these perovskites, as well as the effect on the electrical properties and stability.

2. Experimental

High purity $BaCO_3$ (Aldrich, 99%), $SrCO_3$ (Aldrich, 99.9%), Co_3O_4 (Aldrich), Fe_2O_3 (Fluka, 99%), H_3BO_3 (Aldrich, 99.5%), SiO_2 (Aldrich, 99.6%) and $(NH_4)H_2PO_4$ (Aldrich, 98%) were used to prepare $Ba_{1-y}Sr_yCo_{0.8(1-x)}Fe_{0.2(1-x)}M_xO_{3-\delta}$ (M = B, Si, P; y = 0.5 and 0.67; x = 0, 0.05 and 0.10). The powders were intimately ground and heated initially at 1100 °C for 12 h. They were then ball-milled (350 rpm for 1 h, Fritsch Pulverisette 7 Planetary Mill) and reheated to 1150 °C for a further 12 h. This step was repeated one more time. Hereafter, the $Ba_{1-y}Sr_yCo_{0.8(1-x)}Fe_{0.2(1-x)}M_xO_{3-\delta}$ samples are

* Corresponding author. Tel.: +44 01214148672; fax: +44 01214144403.
  E-mail address: j.m.porras@bham.ac.uk (J.M. Porras-Vazquez).

labeled as $Ba_{1-y}SCFM_x$, where M = B, Si and P; y = 0.05 and 0.67; and x = 0, 0.05 and 0.10.

Since it is known that the parent BSCF system is metastable, the $Ba_{1-y}SCFM_x$ samples were annealed at 750 °C for 144 h in air to study the effect of the P, B-doping on the stability.

Powder X-ray diffraction (Bruker D8 diffractometer with Cu $K\alpha_1$ radiation) was used to demonstrate phase purity, as well as for cell parameter determination. For the latter, the GSAS suite of programs was used [20].
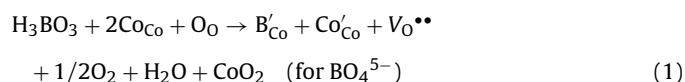
Oxygen contents were estimated from thermogravimetric analysis (Netzsch STA 449 F1 Jupiter Thermal Analyser). Samples were heated at 10 °C min⁻¹ to 1200 °C in N_2 and held for 30 min to reduce the transition metal oxidation state to 3+, with the original oxygen content then being determined from the mass loss observed.

Pellets for conductivity measurements were prepared as follows: the powders were first ball-milled (350 rpm for 1 h), before pressing as pellets and sintering at 1150 °C for 12 h. Conductivities were then measured using the 4 probe dc method. Four Pt electrodes were attached with Pt paste, and then the sample was fired to 800 °C in air for 1 h to ensure bonding to the sample. The samples were then furnace cooled to 350 °C and held at this temperature for 12 h to ensure full oxygenation.
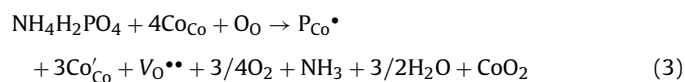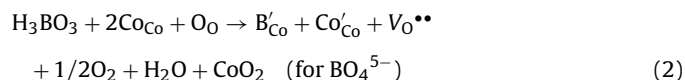
3. Results and discussion

The X-ray diffraction data suggested that the samples were successfully doped up to x = 0.05 for P and B-doping (the XRD patterns for the P-doped samples are shown in Fig. 1). Higher amounts of dopant led to segregation of impurities, such as $Co_2P_4O_{12}$ for P-doping and a small amount of barium ferrite for B-doping. For Si-doping, the segregation of secondary phases, such as $Sr_2CoSi_2O_7$, was observed in all cases. Thus the further characterization work was focused on the B, P doped systems.

Cell parameters were determined from the X-ray diffraction data by the Rietveld method (see Table 1), and no change in symmetry (cubic cell) was observed on doping. The change in cell parameters for these oxyanion doped perovskite materials is a balance between the effect of the smaller size of B^{3+} and P^{5+}, which would be expected to lead to a reduction in cell volume, and the associated reduction of Co/Fe to give a greater concentration of Co^{3+}/Fe^{3+}, which would lead to an increase in cell volume. The formation of 3+ species through these doping strategies is predicted by the following defect equations (assuming replacement of Co; similar equations could be written for replacement of Fe):

$$H_3BO_3 + 2Co_{Co} + O_O \rightarrow B'_{Co} + Co'_{Co} + V_O^{\bullet\bullet}$$
$$+ 1/2O_2 + H_2O + CoO_2 \quad (for\ BO_4^{5-}) \tag{1}$$

or

$$H_3BO_3 + 2Co_{Co} + O_O \rightarrow B'_{Co} + Co'_{Co} + V_O^{\bullet\bullet}$$
$$+ 1/2O_2 + H_2O + CoO_2 \quad (for\ BO_4^{5-}) \tag{2}$$

$$NH_4H_2PO_4 + 4Co_{Co} + O_O \rightarrow P_{Co}^{\bullet}$$
$$+ 3Co'_{Co} + V_O^{\bullet\bullet} + 3/4O_2 + NH_3 + 3/2H_2O + CoO_2 \tag{3}$$

The average oxidation states of Co/Fe were determined from TGA to be 3.64+ and 3.78+ for $Ba_{0.33}SCFP_{0.05}$ and $Ba_{0.5}SCFP_{0.05}$, respectively; and 3.71+ and 3.80+ for $Ba_{0.33}SCFB_{0.05}$ and $Ba_{0.5}SCFB_{0.05}$, respectively. For the undoped compositions, the values were 3.78 and 3.84 for $Ba_{0.33}SCFM_0$ and $Ba_{0.5}SCFM_0$, respectively. For the B-doped samples all cell volumes are slightly smaller than those of the undoped compositions (Table 1). From the defect equations, the lower degree of reduction for the B-doped samples compared to the P-doped samples would suggest incorporation of B

as BO_4^{5-}, and, likely, the small size of B^{3+} counterbalances the effect of this partial reduction of $(Co/Fe)^{4+}$. For the P-doped samples all cell volumes are bigger than those of the undoped compositions, consistent with the greater degree of reduction in this case, outweighing the small size of P^{5+}.

As noted in Section 1, the parent BSCF materials are metastable and will transform to a hexagonal perovskite after long term annealing at intermediate temperatures. In order to examine the effect of phosphate/borate incorporation on this stability, annealing studies in air were performed on both powders and pellets (750 °C for 144 h). In agreement with previous studies the undoped compositions partially transformed to a hexagonal cell [13]. However, the P-doped compositions (x = 0.05) showed a cubic cell after the annealing process (Fig. 1). The heavily doped samples (x = 0.10) also gave similar results. The B-doped compositions were also mainly cubic (Fig. 2), however in these cases the results suggested a small degree of the hexagonal cell after the annealing process, although the levels were not as great as in the undoped compositions (Fig. 1). Therefore, the results indicate that oxyanion doping helps to stabilize the cubic form of BSCF reducing the tendency to transform to a hexagonal cell, a significant result in terms of SOFC/oxygen separation applications.

This stabilization of the cubic perovskite structure can be attributed to partial reduction of $(Co/Fe)^{4+}$ to $(Co/Fe)^{3+}$. There are two driving forces for the partial reduction in the Co oxidation state:

1. In the case of phosphate doping, $(Co/Fe)^{4+}$ is being partially replaced by higher valent P^{5+}.
2. The introduction of $P\ B^{-1}$ on the perovskite octahedral cation site requires the creation of oxygen vacancies to convert the coordination to tetrahedral (as required for PO_4^{3-} or BO_4^{5-}), which in turn leads to a requirement for partial reduction of Co/Fe.

As can be seen from Eqs. (1)–(3), the introduction of phosphate and borate groups will lead to significant reduction of the Co/Fe oxidation state. The stabilization of the cubic perovskite polymorph on borate and phosphate doping can then be related to the increased $(Co/Fe)^{3+}$ level, and hence average octahedral cation size, reducing the tolerance factor. The greater reduction on phosphate doping then leads to greater stability of the cubic phase compared to borate doping. It is also possible that the presence of PO_4^{3-}/BO_4^{5-} units may help to disfavor the presence of face sharing, thus promoting corner sharing and hence the formation of the cubic perovskite.

The conductivities of these compositions are shown in Fig. 3 for P-doping. For $Ba_{0.33}SCFM_0$ and $Ba_{0.5}SCFM_0$, the data showed conductivity values between 35.9 and 29.6 S cm⁻¹ from 600 to 800 °C for the former, and 12.9 and 12.6 S cm⁻¹ from 600 to 800 °C for the latter. On doping with low levels of oxyanions a small increase in conductivity was observed: i.e. for $Ba_{0.33}SCFP_{0.05}$, 40.8–33.0 S cm⁻¹ between 600 and 800 °C; and for $Ba_{0.5}SCFP_{0.05}$, 15.6–15.9 S cm⁻¹; for $Ba_{0.33}SCFB_{0.05}$, 40.2–31.4 S cm⁻¹; for $Ba_{0.5}SCFB_{0.05}$, 17.4–17.0 S cm⁻¹. While the conductivities of these doped samples were higher than those for the undoped system, further increases in P and B content led to a small reduction in conductivity, which may be related to the presence of impurities.

The effect of long term annealing on the conductivity of selected samples was also examined, and after annealing the conductivity was observed to decrease for the parent compounds, due to the partial transformation to the hexagonal phase. In contrast, for the P-doped compositions the conductivity remains practically unaltered (Fig. 2). Thus, this oxyanion doping strategy allows the stabilization of the cubic form of barium strontium cobalt ferrites maintaining unaltered the electric properties of these materials, enhancing their use for long term applications, e.g. cathode for SOFCs or oxygen
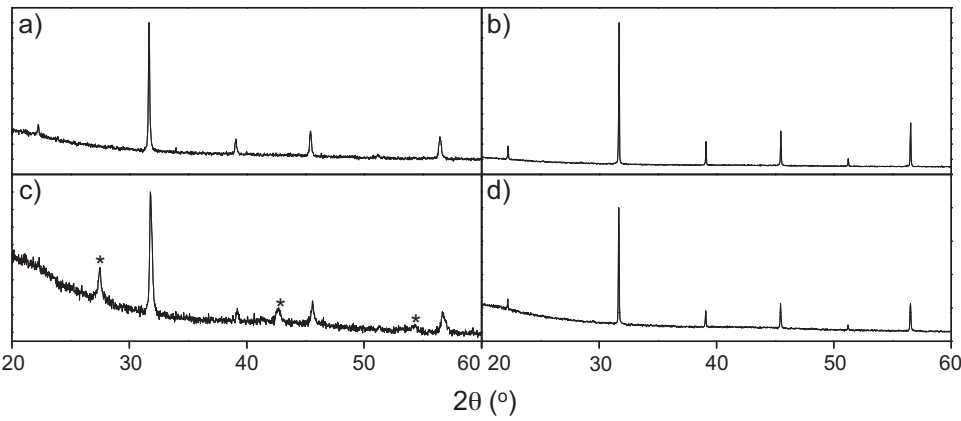
Fig. 1. X-ray diffraction patterns for (a) $Ba_{0.5}Sr_{0.5}Co_{0.8}Fe_{0.2}O_{3-\delta}$ and (b) $Ba_{0.5}Sr_{0.5}Co_{0.76}Fe_{0.19}P_{0.05}O_{3-\delta}$ as prepared; and (c) $Ba_{0.5}Sr_{0.5}Co_{0.8}Fe_{0.2}O_{3-\delta}$ (additional peaks indicating the presence of a hexagonal perovskite highlighted) and (d) $Ba_{0.5}Sr_{0.5}Co_{0.76}Fe_{0.19}P_{0.05}O_{3-\delta}$ annealed at 750 °C for 144 h in air.

Table 1
Cell parameters (cubic cell) for $Ba_{1-y}Sr_yCo_{0.8(1-x)}Fe_{0.2(1-x)}M_xO_{3-\delta}$ (M = B and P; y = 0.5 and 0.67; x = 0 and 0.5).

	$y = 0.5$			$y = 0.67$		
x	0	0.05		0	0.05	
M		B	P		B	P
a (Å)	3.9801(1)	3.9378(1)	3.9867(3)	3.9415(1)	3.9362(1)	3.9456(1)
V (Å^3)	63.05(1)	62.75(1)	63.36(1)	61.23(1)	60.99(1)	61.42(1)
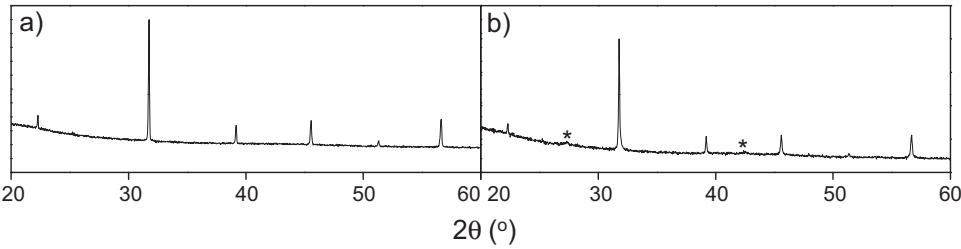
Fig. 2. X-ray diffraction patterns for (a) $Ba_{0.5}Sr_{0.5}Co_{0.76}Fe_{0.19}B_{0.05}O_{3-\delta}$ as prepared and (b) $Ba_{0.5}Sr_{0.5}Co_{0.76}Fe_{0.19}B_{0.05}O_{3-\delta}$ annealed at 750 °C for 144 h in air (additional peaks indicating the presence of a hexagonal perovskite highlighted).
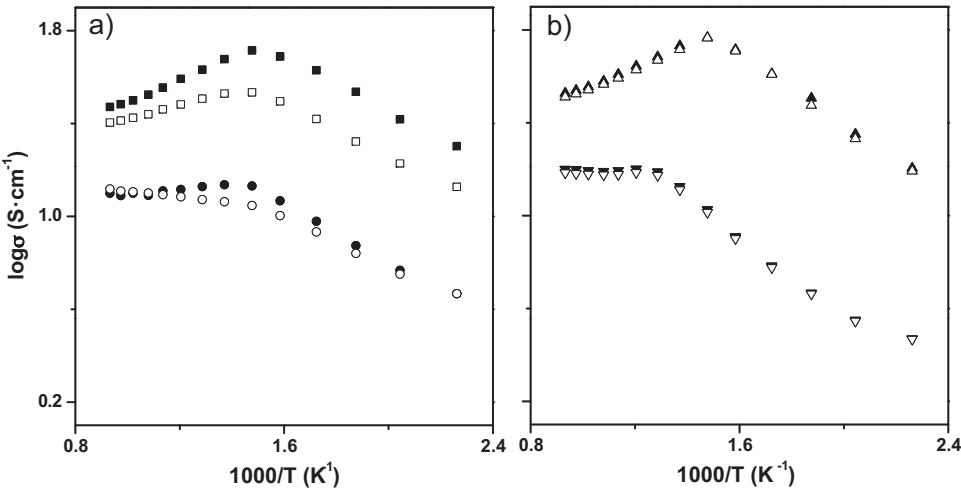

Fig. 3. Arrhenius plots of log σ versus $1000/T$ before (solid symbols) and after (open symbols) annealing for: (a) $Ba_{0.5}Sr_{0.5}Co_{0.8}Fe_{0.2}O_{3-\delta}$ (●, ○) and $Ba_{0.33}Sr_{0.67}Co_{0.8}Fe_{0.2}O_{3-\delta}$ (■, □); and for (b) $Ba_{0.5}Sr_{0.5}Co_{0.76}Fe_{0.19}P_{0.05}O_{3-\delta}$ (▼, ▽) and $Ba_{0.33}Sr_{0.67}Co_{0.76}Fe_{0.19}P_{0.05}O_{3-\delta}$ (▲, △), respectively.

evolution reactions (OER) [21]. Further work is planned to study the performance of these cathode materials with Gd-doped CeO_2 and $LaGaO_3$-based IT electrolytes.

4. Conclusions

Phosphate and borate were successfully incorporated into $Ba_{1-y}Sr_yCo_{0.8(1-x)}Fe_{0.2(1-x)}M_xO_{3-\delta}$ (M = P and B) with a small improvement in the electronic conductivity for low levels of doping. In addition, oxyanion doping helps to improve the stability of the cubic form of barium strontium cobalt ferrites as demonstrated by long term annealing studies at intermediate temperatures, and hence maintain unaltered its electrical properties. Further work is planned to examine the performance of these phases as SOFC cathodes.

Acknowledgments

References

[1] A. Orera, P.R. Slater, Chem. Mater. 22 (2010) 675–690.
[2] S.J. Skinner, Int. J. Inorg. Mater. 3 (2001) 113–121.
[3] J.A.M. Van Roosmalen, E.H.P. Cordfunke, Solid State Ionics 52 (1992) 303–312.
[4] A. Hammouche, E. Siebert, A. Hammou, Mater. Res. Bull. 24 (1989) 367–380.
[5] R.A. De Souza, J.A. Kilner, Solid State Ionics 106 (1998) 175–187.
[6] S.P. Jiang, J. Mater. Sci. 43 (2008) 6799–6833.
[7] H. Yokokawa, T. Horita, in: S.C. Singhal, K. Kendall (Eds.), High Temperature Solid Oxide Fuel Cells: Fundamentals, Design and Applications, Elsevier Advanced Technology, Oxford, UK, 2003.
[8] J.F. Vente, W.G. Haije, Z.S. Rak, J. Membr. Sci. 276 (2006) 178–184.
[9] Z.P. Shao, W.S. Yang, Y. Cong, H. Dong, J.H. Tong, G.X. Xiong, J. Membr. Sci. 172 (2000) 177–188.
[10] H. Wang, Y. Cong, W. Yang, Chem. Commun. (2002) 1468–1469.
[11] Z. Shao, G. Xiong, J. Tong, H. Dong, W. Yang, Sep. Purif. Technol. 25 (2001) 419–429.
[12] Z.P. Shao, S.M. Haile, Nature 431 (2004) 170–172.
[13] S. Švarcová, K. Wiik, J. Tolchard, H.J.M. Bouwmeester, T. Grande, Solid State Ionics 178 (2008) 1787–1791.
[14] J.F. Shin, L. Hussey, A. Orera, P.R. Slater, Chem. Commun. 46 (2010) 4613–4615.
[15] J.F. Shin, D.C. Apperley, P.R. Slater, Chem. Mater. 22 (2010) 5945–5948.
[16] J.F. Shin, P.R. Slater, J. Power Sources 196 (2011) 8539–8543.
[17] J.F. Shin, K. Joubel, D.C. Apperley, P.R. Slater, Dalton Trans. 41 (2012) 261–266.
[18] C.A. Hancock, P.R. Slater, Dalton Trans. 40 (2011) 5599–5603.
[19] C.A. Hancock, R.C.T. Slade, J.R. Varcoe, P.R. Slater, J. Solid State Chem. 184 (2011) 2972.
[20] A.C. Larson, R.B. von Dreele, GSAS program, Los Alamos National Lab. 523, Rep. No. LA-UR-86748, 1994.
[21] J. Suntivich, K.J. May, H.A. Gasteiger, J.B. Goodenough, Y. Shao-Horn, Science 334 (2011) 1383–1385.